

Magnetic Depopulation of 1D Subbands in a Narrow 2D Electron Gas in a GaAs:AlGaAs Heterojunction

K.-F. Berggren,^(a) T. J. Thornton, D. J. Newson, and M. Pepper^(b)

Cavendish Laboratory, Cambridge CB3 0HE, United Kingdom

(Received 12 May 1986)

We present results on the transverse magnetoconductance in the range 0.3 to 8 T of a narrow, variable-width channel in a GaAs:AlGaAs heterojunction. As the width of the channel is decreased below $0.25 \mu\text{m}$ the structure in the magnetoconductance changes from Shubnikov-de Haas oscillations to the magnetic depopulation of one-dimensional subbands. A semiclassical WKB calculation is presented which gives good agreement with experiment.

PACS numbers: 72.20.My, 73.40.Lq

In previous work¹ we have demonstrated the existence of disorder-induced, one-dimensional conductivity corrections in a narrow-channel electron gas within a split-gate GaAs:AlGaAs heterojunction field-effect transistor. At temperatures such that the phase-relaxation (inelastic) length and the interaction length are greater than the channel width, the quantum corrections to the conductivity become one dimensional.^{2,3} Similar effects have been observed in other systems.⁴⁻⁶

In this Letter we present results on the effects of a large, transverse magnetic field on the conductivity when the channel is narrow. A WKB calculation is presented which shows that a magnetic-field-induced depopulation of the one-dimensional subbands occurs. The mobility in this system is much higher than in other quasi 1D systems so that lifetime broadening⁷ of electronic subbands ($\cong \hbar/\tau$) is sufficiently small for subband depopulation to be directly observed as structure in the magnetoconductance. Here τ is the elastic lifetime.

The devices used in this work were similar to those described in Ref. 1 but had an enlarged gate separation of $1.0 \mu\text{m}$ as shown in Fig. 1. The channel width can be extracted from the positive magnetoconductance arising from quantum interference effects.^{1,2} The quantum interference is quenched by a weak magnetic field when the cyclotron length is shorter than the elastic mean free path, leaving only the conductivity correction due to the electron-electron interaction² given by

$$\delta G = - (e^2 \alpha / \pi \hbar) (\hbar D / 2kT)^{1/2}, \quad (1)$$

where α is the 1D interaction parameter^{2,4} and has the value 1.33, and D is the electron diffusion coefficient. The screening parameter F has the value 0.35 in this range. The exchange contribution dominates over the Hartree contribution and hence α does not vary significantly with change in F or carrier concentration.^{2,4}

For channel widths greater than 1000 \AA the value of

$\delta G(B)/G(B=0)$ is so small that the channel width cannot be accurately determined from the quantum interference corrections. However, the width can be independently determined from the temperature-dependent electron-electron interaction correction. In these devices a transverse magnetic field of 0.15 T was sufficient to quench the quantum interference without enhancing the interaction correction ($|g_L \mu B| \ll kT$, where g_L is the Landé g factor and μ is the Bohr magneton), so that the change in the conductivity with temperature depends only upon the electron-electron interaction according to Eq. (1).

The conductance g (G/L , where L is the channel length) was measured in a magnetic field of 0.15 T as a function of temperature and plotted against $T^{-1/2}$. D was determined from the best straight-line fit. Extrapolation to $T^{-1/2} = 0$ gave a value for the Boltzmann conductance given by $g_B = N(E_F) D e^2 t / L$. If we assume a 2D density of states $N(E_F)$ and use the estimate of D obtained from the gradient it is possible to extract the channel width t . We expect the assumption of a 2D density of states to be a good approximation for widths greater than 1000 \AA when several (i.e., more than four) subbands are occupied.

We have measured the magnetoconductance for different channel widths in the temperature range 4.2 to

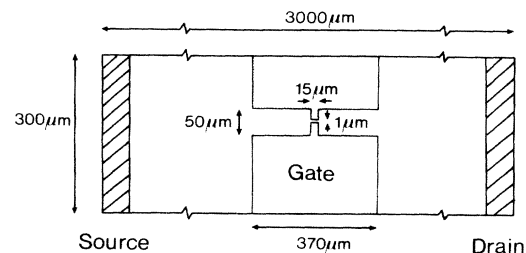


FIG. 1. A schematic diagram of the split-gate heterojunction field-effect transistor used to define a narrow channel in a 2D electron gas.

0.35 K in magnetic fields up to 8 T. The magnetic field strength B was measured with a calibrated Hall probe with a nonlinear response above 1 T. Here we concentrate on these effects found for $B > 0.3$ T. We will report results for lower fields elsewhere. In order to avoid electron heating, the electric field along the channel under the gate was less than 1 V/m and the conductivity was measured by conventional phase-sensitive techniques.

When the narrow-channel resistance is not totally dominant ($V_g > -3.0$ V), the magnetoconductance exhibits two Fourier components. One component corresponds to a carrier concentration of $4.0 \times 10^{11} \text{ cm}^{-2}$ and arises from Shubnikov-de Haas oscillations in the 2D regions between the channel and the source and drain. The other component has a larger period and is due to Shubnikov-de Haas oscillations within the channel itself. The period of these oscillations did not vary as the width was reduced from 10 000 to 2500 Å showing that the carrier concentration within the channel remained constant at $(1.5 \pm 0.1) \times 10^{11} \text{ cm}^{-2}$. The origin of the drop in carrier concentration may be the electron electron-beam lithography. In the calculation presented here we have assumed this concentration for all channel widths.

In order to illustrate the general behavior of the magnetoconductance of the channel as a function of confining voltage we have plotted a fan diagram, Fig. 2. We first point out that as the effective sample aspect ratio is always less than $\frac{1}{30}$ (length = 15 μm, width less than 5000 Å), the maxima in conductance correspond to E_F lying between Landau levels^{8,9} and hence the fan passes through zero index. As observed, the initial decrease in V_G produces no change and the experimental points are coincident. Reduction in the channel width below 2500 Å produces a change in slope and a pronounced curvature from $1/B$ behavior at low values of magnetic field which becomes stronger with decreasing width (plotting minima in conductance also gives the same behavior).

This behavior arises as the perturbation to the Landau levels is not weak and the magnetoconductance oscillations are no longer periodic in $1/B$ (an effect which is most significant at low B), but arise from the successive magnetic depopulation of one-dimensional hybrid electric-magnetic subbands. The effects of a parallel magnetic field on the depopulation of quantized levels in a 2D system is well known.^{10,11} In the present experiment the narrow width of the channel gives rise to 1D subbands and these are forced through the Fermi level by an increasing transverse magnetic field. As each level passes through the Fermi level a sharp change occurs in both the density of states and intersubband scattering, which, in an ideal system, results in a discontinuity in the conductance.⁷ We have calculated the magnetic depopulation of the sub-

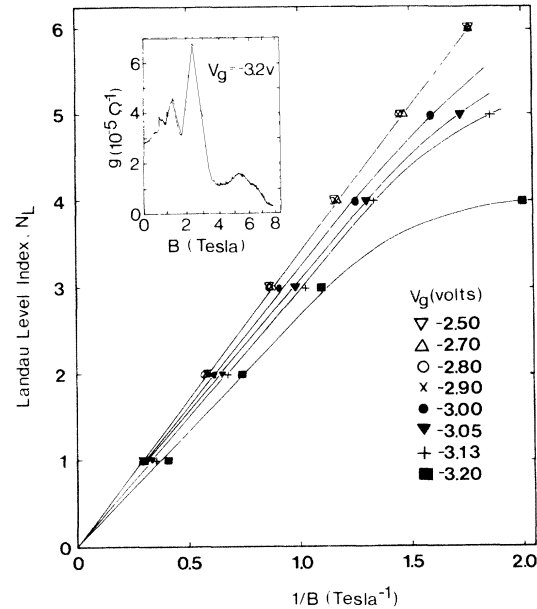


FIG. 2. A fan diagram showing the conductance maxima plotted as a function of reciprocal magnetic field. For channel widths $5000 \text{ Å} \geq t > 2500 \pm 200 \text{ Å}$ ($-2.5 \text{ V} \geq V_g > -3.0 \text{ V}$) the points are coincident but for widths $2500 \text{ Å} \geq t \geq 1500 \pm 200 \text{ Å}$ ($-3.0 \text{ V} \geq V_g \geq -3.2 \text{ V}$) there is a pronounced departure from $1/B$ behavior. The deviation cannot be explained by the uncertainty in the magnetic field which is typically 5%. Inset: Magnetoconductance oscillations for a channel of width $1500 \pm 200 \text{ Å}$ ($V_g = -3.2 \text{ V}$) at a temperature of 0.35 K. The widths were determined as described in the text.

bands in the following way.

The confinement of the electrons to a potential well gives rise to sublevel quantization of the motion across the well, while the motion along the channel remains free-electron-like. Although a "particle in a box" model may be a more realistic description of the present situation, the physics associated with the application of a magnetic field is brought out more clearly by means of the following exactly solvable model. Let the electrons be confined to the parabolic well

$$V_0(x) = m^* \omega_0^2 x^2 / 2, \quad (2)$$

where ω_0 is a characteristic frequency. Then the sublevels are $E_n = \hbar \omega_0 (n + \frac{1}{2})$. With addition of the translational motion the one-electron energies are $E_n(k) = E_n + \hbar^2 k^2 / 2m^*$. If we ignore lifetime broadening due to disorder the one-dimensional density of states associated with the n th subband is consequently

$$N_n(E) = \frac{1}{\pi \hbar} [2m^* / (E - E_n)]^{1/2} \theta(E - E_n); \quad (3)$$

$\theta(x)$ is the Heaviside step function.

If a magnetic field B is applied perpendicular to the

interface an electron of momentum \mathbf{k} experiences an additional confinement through the "magnetic" parabola¹²

$$V_B(x) = m^* \omega_c^2 (x - x_0)^2 / 2, \quad (4)$$

where ω_c is the cyclotron frequency and $x_0 = \hbar kc / (eB)$. Added together $V_0(x)$ and $V_B(x)$ give rise to a shifted parabola with a new characteristic frequency $\omega = (\omega_0^2 + \omega_c^2)^{1/2} > \omega_0$. The one-electron energies are now $E_n(k) = E_n(B) + \hbar^2 k^2 / 2m^*(B)$, where $E_n(B) = \hbar \omega (n + \frac{1}{2})$ and $m^*(B) = m^* \omega^2 / \omega_0^2 > m^*$ is an effective "magnetic" mass. The magnetic field thus acts in two ways: The separation of the sublevels, ΔE , increases and the electrons appear heavier resulting in a flattening of the subband dispersions. Because ΔE increases with B the subbands successively depopulate. This process is accelerated by the simultaneous change in the density of states, Eq. (3), in which m^* and E_n are to be replaced by $m^*(B)$ and $E_n(B)$. $N_n(E)$ thus becomes more sharply peaked in the presence of a magnetic field with a greater possibility of our observing structure due to subband population.

As mentioned, the parabolic potential in Eq. (2) gives qualitatively the correct physics, but is not expected to be numerically accurate in the present context. The true potential is, however, hard to assess because of the possibility of charged defects in the AlGaAs introduced during processing, as well as the awkward geometry. We therefore model the true confining potential as

$$V(x) = m^* \omega_0^2 (|x| - t/2)^2 / 2 \quad (5)$$

for $|x| > t/2$ and zero otherwise. For ω_0 we choose¹³ $\omega_0^2 = e^2 n_D / \epsilon_s m^*$, where n_D is the doping concentration in the AlGaAs n region and ϵ_s the background dielectric screening constant (12.8). The final results are, however, not sensitive to the choice of ω_0 , provided that t is large ($> 1000 \text{ \AA}$). Using the semiclassical WKB^{12,13} method we find in this case that the sublevels closely approximate the low-lying energy spectrum for a particle in a box, i.e., the flat region of the potential is dominant. Calculated results are shown in the inset of Fig. 3, showing that five subbands are occupied at $B=0$, for a channel width $t = 1500 \text{ \AA}$. We note that the form of the potential is similar to recent numerical calculations in Si metal-oxide semiconductor field-effect transistors.¹⁴ Adding the magnetic potential in Eq. (4) to Eq. (5) the WKB method results in the magnetically perturbed subbands shown in the inset of Fig. 3. The number of occupied subbands is now four. On further increase of B the remaining subbands depopulate leaving only the ground subband occupied when $B > 2.6 \text{ T}$. The flat portion of $E_0(k)$ in the lower inset of Fig. 3 corresponds to Landau orbits located inside the well. At higher fields the remaining

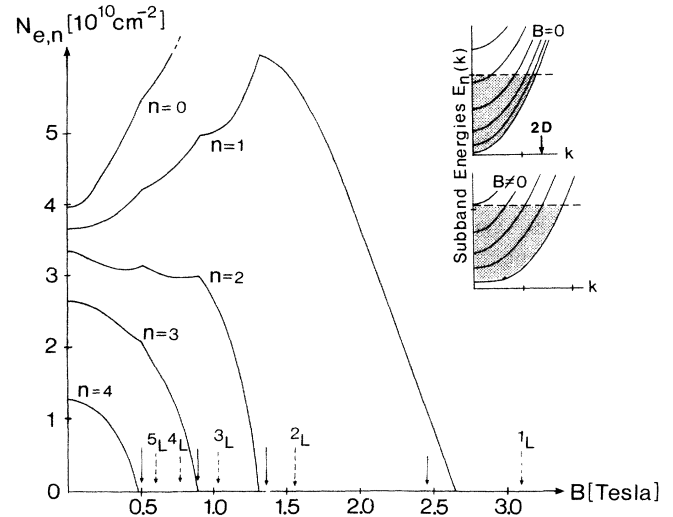


FIG. 3. The calculated number of electrons per unit area occupying the n th subband. Dashed arrows labeled n_L mark the field at which Landau levels in the ideal 2D gas depopulate. Full drawn arrows indicate the fields at which peaks occur in the conductance of Fig. 2(a). In all calculations we have assumed $m^* = 0.067 m_0$, $n_D = 2 \times 10^{17} \text{ cm}^{-3}$, $N_e = 1.5 \times 10^{11} \text{ cm}^{-2}$, and zero temperature. Inset: Calculated subband dispersions, $E_n(k)$, for a channel of width $t = 1500 \text{ \AA}$. The shading indicates occupied states and the horizontal dashed line the Fermi energy. For $B=0 \text{ T}$ (upper curve) the channel is effectively 2D. The arrow labeled 2D marks the position of the Fermi wave number, $k_F(2D) = (2\pi N_e)^{1/2}$, of an ideal 2D gas. The lower case refers to $B=0.5 \text{ T}$. The graph shows how a magnetic field induces a magnetic depopulation because of the increased separation and distortion of the subbands. For $B \geq 2.6 \text{ T}$ only the ground subband remains occupied, i.e., $k_F(1D) = \pi t N_e / 2$.

$E_n(k)$ also acquire dispersionless regions centered around $k=0$. Strong dispersion outside these regions is associated with edge states, i.e., magnetic states interacting heavily with the confining walls. With increasing B (or t) the number of occupied edge states decreases.

The calculated Fermi energy has cusps associated with the depopulation of the hybrid electric-magnetic subbands, and these move to lower fields with decreasing t in qualitative agreement with the shift in peak position illustrated in Fig. 2. Figure 3 shows the number of electrons per subband as a function of B . The fields at which pure Landau levels depopulate are indicated, as well as the position of observed peaks in the conductance observed for a width of 1500 \AA . The theory agrees with experiments in two important aspects. The depopulation of the subbands occurs at fields very close to the occurrence of peaks in the measured conductance. The number of peaks is consistent with the number of initially occupied subbands. We note that the change in the slope of the linear region in Fig. 2

may be affected by a reduction in carrier concentration, but the curvature cannot arise in this way and must reflect the increasingly hybrid nature of the levels.

This work was supported by the Science and Engineering Research Council (United Kingdom) (SERC) and, in part, by the European Research Office of the U.S. Army. One of us (K.-F.B.) acknowledges partial financial support from the Swedish Natural Science Research Council. One of us (T.J.T.) acknowledges an SERC CASE award with GEC and another (D.J.N.) acknowledges an SERC studentship. We wish to thank our collaborators I. Vagner and H. Ahmed of the Cavendish Laboratory and D. Andrews and G. J. Davies of British Telecom Research Centre.

^(a)Permanent address: IFM, Linköping University, Linköping, Sweden.

^(b)Also at GEC Hirst Research Centre, Wembley, Middlesex, United Kingdom.

¹T. J. Thornton, M. Pepper, H. Ahmed, D. Andrews, and

G. J. Davies, *Phys. Rev. Lett.* **56**, 1198 (1986).

²B. L. Altshuler and A. G. Aronov, in *Electron-Electron Interactions in Disordered Systems*, edited by A. L. Efros and M. Pollak (North-Holland, Amsterdam, 1985).

³E. Abrahams, P. W. Anderson, D. C. Licciardello, and T. V. Ramakrishnan, *Phys. Rev. Lett.* **42**, 673 (1979).

⁴K. K. Choi, D. C. Tsui, and S. C. Palmateer, *Phys. Rev. B* **32**, 5540 (1985).

⁵W. J. Skocpol, L. D. Jackel, E. L. Hu, R. E. Howard, and L. A. Fetter, *Phys. Rev. Lett.* **49**, 951 (1982).

⁶C. C. Dean and M. Pepper, *J. Phys. C* **15**, L1287 (1982).

⁷D. G. Cantrell and P. N. Butcher, *J. Phys. C* **18**, 5111 (1985).

⁸S. Kawaji, *Surf. Sci.* **73**, 46 (1978).

⁹T. G. Powell, C. C. Dean, and M. Pepper, *J. Phys. C* **17**, L359 (1984).

¹⁰F. Koch, in *High Magnetic Fields*, edited by S. Chikazumi and N. Miura (Springer-Verlag, Berlin, 1981), p. 262.

¹¹D. J. Newson, K.-F. Berggren, M. Pepper, H. W. Myron, G. J. Davies, and E. G. Scott, *J. Phys. C* **19**, L403 (1986).

¹²L. D. Landau and E. M. Lifshitz, *Quantum Mechanics* (Pergamon, Oxford, U.K., 1975), 2nd ed.

¹³D. A. Poole, M. Pepper, K.-F. Berggren, G. Hill, and H. W. Myron, *J. Phys. C* **15**, L21 (1982).

¹⁴S. Laux and F. Stern, *Appl. Phys. Lett.* **49**, 91 (1986).

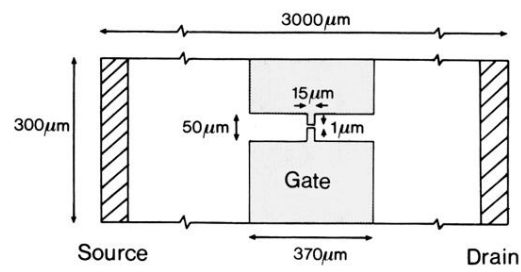


FIG. 1. A schematic diagram of the split-gate heterojunction field-effect transistor used to define a narrow channel in a 2D electron gas.

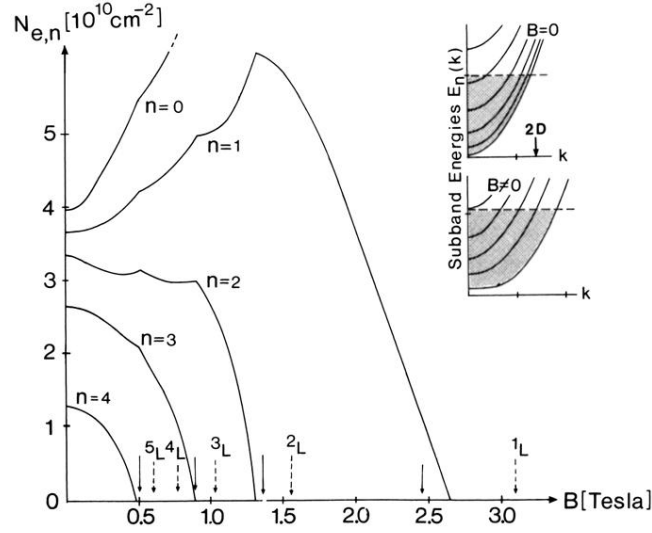


FIG. 3. The calculated number of electrons per unit area occupying the n th subband. Dashed arrows labeled n_L mark the field at which Landau levels in the ideal 2D gas depopulate. Full drawn arrows indicate the fields at which peaks occur in the conductance of Fig. 2(a). In all calculations we have assumed $m^* = 0.067 m_0$, $n_D = 2 \times 10^{17} \text{ cm}^{-3}$, $N_e = 1.5 \times 10^{11} \text{ cm}^{-2}$, and zero temperature. Inset: Calculated subband dispersions, $E_n(k)$, for a channel of width $t = 1500 \text{ \AA}$. The shading indicates occupied states and the horizontal dashed line the Fermi energy. For $B = 0 \text{ T}$ (upper curve) the channel is effectively 2D. The arrow labeled 2D marks the position of the Fermi wave number, $k_F(2D) = (2\pi N_e)^{1/2}$, of an ideal 2D gas. The lower case refers to $B = 0.5 \text{ T}$. The graph shows how a magnetic field induces a magnetic depopulation because of the increased separation and distortion of the subbands. For $B \geq 2.6 \text{ T}$ only the ground subband remains occupied, i.e., $k_F(1D) = \pi t N_e / 2$.